Proc. Natl. Acad. Sci. USA
Vol. 90, pp. 8929–8933, October 1993
Biochemistry

Site-specific and compensatory mutations imply unexpected pathways for proton delivery to the Q_B binding site of the photosynthetic reaction center

(proton transfer/photosynthesis/suppressor mutations/electron transfer/membrane protein)

DEBORAH K. HANSON*†, DAVID M. TIEDE‡, SHARRON L. NANCE*, CHONG-HWAN CHANG*§, AND MARIANNE SCHIFFER*

*Biological and Medical Research Division and ‡Chemistry Division, Argonne National Laboratory, Argonne, IL 60439

Communicated by R. Haselkorn, June 21, 1993 (received for review March 12, 1993)

ABSTRACT **In photosynthetic reaction centers, a quinone molecule, Q_B, is the terminal acceptor in light-induced electron transfer. The protonatable residues Glu-L212 and Asp-L213 have been implicated in the binding of Q_B and in proton transfer to Q_B anions generated by electron transfer from the primary quinone Q_A. Here we report the details of the construction of the Ala-L212/Ala-L213 double mutant strain by site-specific mutagenesis and show that its photosynthetic incompetence is due to an inability to deliver protons to the Q_B anions. We also report the isolation and biophysical characterization of a collection of revertant and suppressor strains that have regained the photosynthetic phenotype. The compensatory mutations that restore function are diverse and show that neither Glu-L212 nor Asp-L213 is essential for efficient light-induced electron or proton transfer in *Rhodobacter capsulatus*. Second-site mutations, located within the Q_B binding pocket or at more distant sites, can compensate for mutations at L212 and L213 to restore photocompetence. Acquisition of a single negatively charged residue (at position L213, across the binding pocket at position L225, or outside the pocket at M43) or loss of a positively charged residue (at position M231) is sufficient to restore proton transfer activity to the complex. The proton transport pathways in the suppressor strains cannot, in principle, be identical to that of the wild type. The apparent mutability of this pathway suggests that the reaction center can serve as a model system to study the structural basis of protein-mediated proton transport.**

The reaction center (RC) in the photosynthetic membrane mediates light-initiated redox chemistry, producing a transmembrane charge separation (for review, see ref. 1). The RC from purple bacteria is the first integral membrane protein complex for which an atomic structure has been determined (1–4). Thus, the RC currently serves as the best model for understanding protein-mediated electron transfer and the subsequent transfer of protons from the aqueous phase to buried protein sites.

The RC is a complex of three protein subunits, the intermembrane L and M chains and the H polypeptide, as well as several cofactors (four bacteriochlorophylls, two bacteriopheophytins, two quinones, and a nonheme iron atom). The cofactors are chemically active in light-induced electron transfer (for review, see ref. 5) and the detailed contribution of the protein to the electrochemistry of this process is obscure. An approximate two-fold symmetry relates the L and M subunits and their cofactors, suggesting two possible routes of charge separation across the photosynthetic membrane. However, normal photochemistry follows only the pathway that is primarily associated with the L subunit. Upon light activation, an electron is transferred from the "special pair" bacteriochlorophyll dimer (P) to the L-side bacteriopheophytin. The final steps involve electron transfer from the primary quinone (Q_A) to the secondary quinone (Q_B) near the cytoplasmic face of the membrane (1, 2, 5, 6).

Although Q_A and Q_B in the RCs of *Rhodobacter (Rb.) capsulatus* and *Rhodobacter sphaeroides* are identical ubiquinone$_{10}$ molecules, their binding sites and *in situ* chemical properties are quite different (7). As the primary quinone acceptor, Q_A receives only a single electron from bacteriopheophytin and does not become protonated; the electron is transferred from Q_A to Q_B in 20–200 μs. Q_B, however, accepts two electrons from successive light-induced turnovers of Q_A. Although it has no contact with the aqueous environment, Q_B^{2-} gains two protons from the cytoplasm, forming Q_BH_2, which diffuses out of the RC (8) and is replaced by a quinone from the membrane pool; Q_BH_2 is reoxidized by the cytochrome bc_1 complex.

Clearly, aspects of the protein structure influence both the chemical properties of the quinones and the electrostatics of photoinitiated electron and proton transfer. The Q_B binding pocket is significantly more polar than that of Q_A in the species whose RC sequences are known [the above plus *Rhodopseudomonas (Rp.) viridis, Rhodospirillum (Rs.) rubrum*, and *Chloroflexus aurantiacus*]. The most striking difference is that residues M246 and M247 in the Q_A site are conserved hydrophobic alanines in all but *C. aurantiacus* (9–16), while the equivalent residues in the Q_B site are always either acidic or polar (Glu-L212 and Asp/Asn-L213). Glu-L212 and Asp-L213 have been shown to be components of the pathway(s) for proton transfer to Q_B in wild-type *Rb. sphaeroides* (17–20).

In this paper, we describe the construction and report additional characteristics of a site-specific double mutant of *Rb. capsulatus*, Glu-L212/Asp-L213 → Ala-L212/Ala-L213 (L212-213AA). This strain is incapable of photosynthetic growth. We also report the genetic characterization of a surprising array of photocompetent derivatives of this double mutant strain and a description of some of the biophysical properties of their RCs. These strains carry reversions or second-site suppressor mutations, some at distant sites, which restore electron and proton transfer to RCs that lack one or both acidic residues at L212 and L213. The spectrum of mutations carried by these strains demonstrates that there can be multiple possible pathways for the delivery of protons to the Q_B site within the protein framework of the RC.

The publication costs of this article were defrayed in part by page charge payment. This article must therefore be hereby marked "*advertisement*" in accordance with 18 U.S.C. §1734 solely to indicate this fact.

Abbreviations: RC, reaction center; P, "special pair" bacteriochlorophyll dimer; Q_A, primary quinone; Q_B, secondary quinone.

†To whom reprint requests should be addressed.
§Present address: DuPont Merck Pharmaceutical Co., DuPont Experimental Station, P.O. Box 80228, Wilmington, DE 19880-0228.

MATERIALS AND METHODS

Structure Analysis. Quinone binding sites were modeled by examining the *Rb. sphaeroides* RC structure (3, 4) with the program FRODO (21). The residue numbering of *Rb. capsulatus* (9) was used; alignments are those as suggested (12–15).

Mutant Construction. The system of plasmids described by Bylina *et al.* (22, 23) was used for site-specific mutagenesis according to a kit (Bio-Rad) based on the method of Kunkel *et al.* (24). The *Hin*dIII–*Kpn* I fragment carrying residues 1–253 of the *L* gene was subcloned into bifunctional vector pBS$^+$/− (Stratagene) and mutagenized with a 30-mer containing two single-base changes at L212 and L213. *Escherichia coli* colonies harboring mutant plasmids were detected by hybridization with the end-labeled oligonucleotide (25). The mutations were verified by dideoxynucleotide sequencing of double-stranded DNA (Sequenase, United States Biochemical). The mutant *L* gene was returned to the *puf* operon in plasmids pU29 (22) and pU2922 (23). Mutant plasmids were transferred to *Rb. capsulatus* deletion strain U43, which lacks light-harvesting and RC complexes (26), by conjugation with *E. coli* donor strain S17-1 (27). *Rb. capsulatus* transconjugants were selected by dark aerobic culture on RCV agar (28) and purified on MPYE agar (29). Plasmids were selected by kanamycin (30 μg/ml). The "wild-type" is U43 complemented in trans by plasmid pU2922.

The double mutant (U43[pR212AA]) was propagated under chemoheterotrophic growth conditions (semiaerobic, dark, 34°C) on RPYE medium (30) to avoid selective pressure for functional RCs. To determine the photosynthetic growth phenotype, MPYE agar was spotted with 2 μl of strains grown chemoheterotrophically and then incubated under a light intensity of 25 W/m^2 in anaerobic jars (Gaspack systems; BBL). Spots of mutant, wild-type, and deletion strains were evaluated within 2 days to exclude the possible contribution of revertants to the observed phenotype (31).

Isolation and Genetic Characterization of Revertants. Photocompetent (PS$^+$) derivatives of the L212-213AA mutant were selected under photosynthetic conditions by incubating plates spread with a chemoheterotrophically grown culture of this strain. Revertants were purified through two subsequent rounds of photosynthetic culture, after which cultures for analysis were grown chemoheterotrophically to eliminate selection for additional reversion events. Plasmids were recovered from the revertants and reconjugated into the deletion strain to determine whether the PS$^+$ phenotype cotransferred with the plasmid. In the photosynthetic growth assay (see above) for cotransfer, samples of these "reconstructed" strains were evaluated by comparison to the original revertant strains. The *L* and *M* gene segments were subcloned into the pBS$^+$/− vector for sequencing.

To map the compensatory mutations, combinations of revertant and wild-type *puf* operon segments were engineered by exploiting the unique restriction sites present in plasmid pU29 (ref. 22, see also ref. 32). Revertant *L* or *M* genes were shuttled into tagged versions of pU29 or pU2922 (*Bal* I, codons L181 and L182; *Bgl* II, codon M86). Switching of segments was monitored by screening for loss of the appropriate restriction site. Chimeric plasmids were returned to *Rb. capsulatus* via conjugation, and the photocompetence of these strains was determined as described above. Strains that grew vigorously within 2 days were scored PS$^+$.

Photosynthetic growth rates in liquid culture were determined by using dark-grown cultures to inoculate tubes filled completely with RCV/kan medium. After overnight dark incubation, tubes were illuminated continuously (25 W/m^2). Turbidities were measured with a Klett–Summerson colorimeter (no. 66 filter).

Kinetic Measurements of Electron Transfer Rates. Chromatophores were prepared (33) from chemoheterotrophic cultures of "reconstructed" PS$^+$ derivatives and the wild-type and double-mutant strains. Single-wavelength transients were measured at room temperature with a single-beam spectrometer of local design (conditions in figure legends). Probe light from a 50-W tungsten lamp was passed through a monochrometer, focused upon the sample, then collected, and passed through a second monochrometer before detection with an avalanche photodiode (RCA). Flash excitation was provided by a 20-nsec 590-nm pulse of 1.5 mJ/cm^2 from a frequency-doubled yttrium/aluminum garnet (YAG)-pumped rhodamine dye laser. Between flashes, the sample was kept dark. An electronic shutter blocked the measuring beam until immediately prior to the kinetic measurement. Absorbance transients were fitted as the sum of multiple exponentials with a Marquardt nonlinear least-squares fitting program provided by Seth Snyder (Argonne National Laboratory).

RESULTS

Double Mutant L212-213AA. The positions of the Glu-L212 and Asp-L213 residues are shown in Fig. 1. The L212-213AA mutant, which carries two single-base-pair mutations, is incapable of photosynthetic growth (PS$^-$; Table 1). Optical and electron paramagnetic resonance spectra showed RCs that display wild-type characteristics (M. C. Thurnauer, Y. Zhang, and D.K.H., unpublished data), and the initial electron transfer rate is similar to that of the wild type (34). These

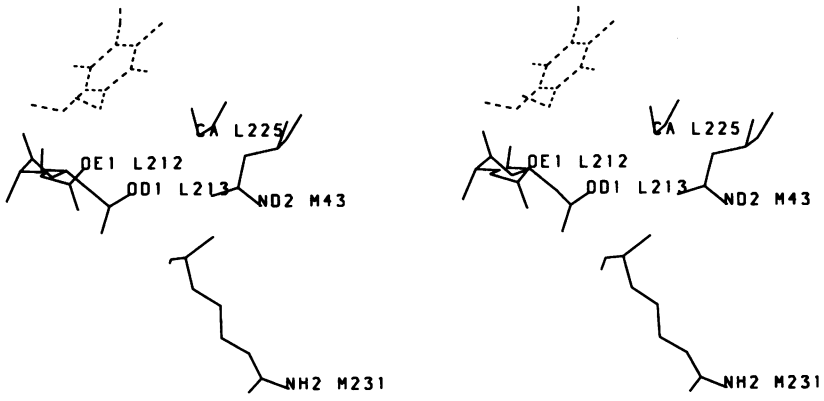

FIG. 1. Stereo molecular model, using the *Rb. sphaeroides* structure (3), of the relative positions of residues near Q_B (dashed lines) in the wild type—Glu-L212, Asp-L213, Gly-L225, Asn-M43, and Arg-M231. Sequence alterations at these sites in mutant, revertant, and suppressor strains are described in the text. Arg-M231 is involved in conserved ion-pair interactions with Glu-H125 and Glu-H232 (see ref. 30). Numbers refer to the *Rb. capsulatus* sequence (9).

Table 1. Revertants and suppressors of the L212-213AA mutant

Strain	Amino acid residue					Doubling time·PS⁺ growth, hr
	L212	L213	L225	M43	M231	
Wild type	Glu	Asp	Gly	Asn	Arg	4.9
Double mutant	Ala	Ala	Gly	Asn	Arg	>168
PS⁺ derivative						
Class 1 rev	Ala	Asp	Gly	Asn	Arg	5.3
Class 2 sup	Ala	Ala	Asp	Asn	Arg	6.5
Class 3 sup	Ala	Ala	Gly	Asn	Leu	6.8
Class 4 sup	Ala	Ala	Gly	Asp	Arg	6.0
Class 5 sup	Ala	Ala	Gly	Asn	Arg	ND

Class 5 has a chromosomal suppressor (sup); all other mutations are plasmid borne. ND, not determined; rev, revertant.

data show that the double mutant assembles RCs that function normally in primary charge separation events.

Isolation of Revertants and Suppressors of the L212-213AA Double Mutation. After long-term incubation of plates under photosynthetic conditions, photocompetent derivatives of the L212-213AA mutant were selected. Several nonindependent PS⁺ strains were purified. Genetic and sequence characterization has thus far grouped them into five classes. Classes 1–4 carry plasmid-borne compensatory mutations (Table 1). In class 5 strains, the compensatory mutation(s) is chromosomal and has not yet been characterized. None of the events replaced Ala-L212. Our results show that there is no absolute requirement for polar residues at either L212 or L213.

Genetic Characterization of Revertants and Suppressors. *Class 1.* Only class 1 carries a reversion of one of the site-specific mutations, a GCC → GAC transversion at L213 (Ala → Asp; Table 1). Ala-L212 is still present.

Class 2. This class retains the site-specific L212 and L213 mutations and carries an intragenic suppressor at L225. A GGC → GAC transition substituted Asp for Gly at this site in the loop before the E helix, opposite L212-L213 in the binding pocket (Fig. 1). Modeling of the Asp-L225 substitution showed that its oxygen atoms could occupy essentially the same space in the Q_B pocket as those of Asp-L213.

For each class of PS⁺ derivatives, chimeric plasmids were constructed that established, by complementation, which segments of plasmid DNA were both necessary and sufficient to restore photocompetence (see also ref. 32). For classes 1 and 2, the *L* gene carrying the above mutations was sufficient to confer photocompetence when combined with a wild-type *M* gene. Since photocompetence is a plasmid-borne trait (Table 1), there is no possibility that these strains bear other compensatory mutations in the *H* gene. Thus, the above mutations can be directly correlated with the restoration of the PS⁺ phenotype.

Class 3. Sequence and complementation analysis has shown that class 3 strains retain the L212-213AA mutations and carry an intergenic suppressor at M231 (Fig. 1). A CGC → CTC transversion substituted Leu for Arg at this position. Chimeric plasmids that coupled the *L* gene from these strains (i.e., L212-L213AA) with the wild-type *M* gene did not confer the PS⁺ phenotype when transferred to the deletion strain. The PS⁺ phenotype was observed with plasmids that combined both the *L* and *M* genes isolated from these strains with the rest of the wild-type operon, confirming that the Arg-M231 → Leu substitution compensates for the loss of Glu-L212 and Asp-L213.

Class 4. A second type of amino acid replacement in the *M* gene, at residue M43 (Fig. 1), also can act effectively to restore function to RCs carrying the L212-213AA substitutions. Sequence analysis and complementation mapping demonstrated that the Asn-M43 → Asp replacement results in intergenic suppression of the PS⁻ double-mutant phenotype (32).

Kinetics of $Q_A^-Q_B \rightarrow Q_AQ_B^-$ Electron Transfer. The kinetics of $P^+Q_A^-Q_B \rightarrow P^+Q_AQ_B^-$ electron transfer were determined in chromatophores by measuring absorbance transients in the region of 700–900 nm (35–37). Q_A^- and Q_B^- induce different shifts in the optical spectra of RC pigments (35, 36). Electrochromic shifts associated with Q_A^- and Q_B^- formation in *Rb. capsulatus* chromatophores (37) are nearly equivalent to those measured in *Rb. sphaeroides* (35, 36). An isosbestic point for the formation of Q_A^- occurs near 760 nm, providing a convenient wavelength for monitoring Q_B^- formation (35–37). In *Rb. capsulatus* chromatophores, P^+ also contributes to the absorbance transients at this wavelength (37). However, the kinetics for formation of P^+ necessarily differ from those of Q_B^-, and the contribution of P^+ can be removed by subtracting normalized absorbance transients measured in the P absorption bands (37).

Fig. 2*A* shows 760-nm transients in the wild type and in the L212-213AA mutant, corrected for the instantaneous rise and slow decay of P^+ (37). To various extents, the kinetics were biphasic, with the major component displaying a time constant of 20 μs in the wild type. The relatively rapid (250 μs) decay of this transient seen in the wild type on the longer time scale (Fig. 2*A*) is part of a relaxation process that includes proton movement after Q_B^- formation (37). No reaction on the microsecond time scale was detected for the double mutant. Slower transients suggesting a reaction time of ≈6 ms were detected (Fig. 2*A*). This rate is similar to that seen in Asp-L213 → Asn mutants of *Rb. sphaeroides* but slow compared to the Gln-L212/Asn-L213 mutants of that species (19, 20). A complete description of the $Q_A^-Q_B \leftrightarrow Q_AQ_B^-$ equilibrium in the L212-213AA double mutant will be presented elsewhere.

In contrast to the double mutant, the $P^+Q_A^-Q_B \rightarrow P^+Q_AQ_B^-$ reactions in the PS⁺ revertant/suppressor strains occur on the microsecond time scale (Fig. 2*B*). The time constants for the class 3 (38 μs) and class 4 (28 μs) suppressors most closely resemble that of the wild type. No relaxation processes on the 400-μs time scale were detected at this wavelength in the PS⁺ derivatives (Fig. 2*B*).

$Q_A^-Q_B^- \rightarrow Q_AQ_BH_2$ Electron Transfer. Proton delivery has been shown to be the obligatory rate-limiting step in $Q_A^-Q_B^- \rightarrow Q_AQ_BH_2$ electron transfer (for review, see ref. 20). The redox cycling of Q_B into and out of the anion state can be detected by monitoring Q^- absorption at 450 nm, following P^+ reduction by exogenous donors (35, 36). Starting from the Q_AQ_B state, a single flash generates Q_B^- and a net increase in

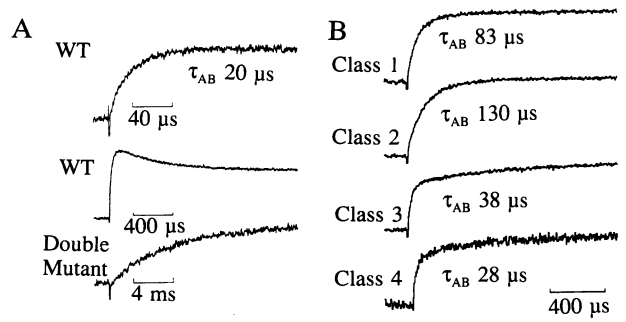

FIG. 2. $P^+Q_A^-Q_B \rightarrow P^+Q_AQ_B^-$ electron transfer kinetics measured by optical transients at 760 nm corrected for contributions due to P^+ (37) (τ_{AB} is the inverse of the first-order rate constant for this reaction). Chromatophores were suspended in 10 mM Tris·HCl (pH 7.8) and adjusted to A_{802} = 0.4–0.5. (*A*) Wild-type (WT, top and middle traces) and L212-213AA double mutant (bottom trace). (*B*) Class 1–4 revertant and suppressor strains. Traces are the average of 8–16 transients, measured with a separation of 25 s between actinic flashes.

absorbance at 450 nm after P^+ has been reduced; the 450-nm signal disappears with electron transfer from $Q_A^-Q_B^- \rightarrow Q_AQ_BH_2$ after a second flash. The resulting binary oscillations in 450-nm absorbance provide an assay to monitor both electron and proton transfer in the $Q_A^-Q_B^- \rightarrow Q_AQ_BH_2$ reaction.

Binary oscillations were observed in the wild type between pH 6 and pH 9 (Fig. 3*A*). In contrast, oscillations were not seen in the L212-213AA double mutant in this same pH range. The observation of a net increase in absorption at 450 nm after the first flash in the L212-213AA strain is consistent with the ability to form a trapped Q_B^- state. However, the lack of a decrease in this absorbance with subsequent flashes, even at pH 6 (not shown), indicates that the $Q_A^-Q_B^- \rightarrow Q_AQ_BH_2$ reaction is inhibited, presumably because protons cannot be delivered to Q_B during the lifetime of the $Q_A^-Q_B^-$ state. Similar results were obtained with isolated RCs of this double mutant, where quinone binding and Q_B^- formation have been demonstrated (30). The same observations have been made for the Gln-L212/Asn-L213 mutants of *Rb. sphaeroides*, which are defective in proton transfer (19, 20).

All of the PS^+ revertant/suppressor strains completed the $Q_A^-Q_B^- \rightarrow Q_AQ_BH_2$ reaction as indicated by detection of binary 450-nm oscillations. These oscillations were observed at pH 7.8 in the strains of classes 1–3; a representative trace (class 3) is shown in Fig. 3*A*. Oscillations could be observed only at pH $\leq$7 in the class 4 strain (Fig. 3*B*), suggesting that the pK value of its rate-limiting proton donor is shifted to near 7 as compared to a pK value of 9 in the wild type. Steady-state cytochrome *c* oxidation experiments corroborated the above data (data not shown). Both assays demonstrate that the $Q_A^-Q_B^- \rightarrow Q_AQ_BH_2$ reaction is inhibited in the double mutant but is restored in the PS^+ derivatives.

DISCUSSION

Takahashi and Wraight (18, 19) and Paddock *et al.* (38) have proposed models for the sequence of photoinduced protonation steps at the Q_B site. They suggested that the primary proton donor to the Q_B anion(s) is Ser-L223, which is within hydrogen-bonding distance of Q_B. This residue, which is not in contact with the cytosol, is thought to be replenished through a network of proton donors that connects the Q_B site in the interior of the protein with the aqueous environment (for review, see ref. 20).

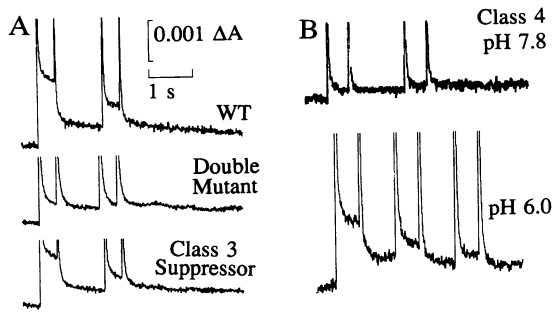

FIG. 3. Absorbance transients measured at 450 nm in the presence of an electron donor, 300 μM ferrocene, to P^+. Chromatophores were suspended to $A_{450} = 1$. (*A*) Wild-type (top trace), L212-213AA double mutant (middle trace), and class 3 suppressor (bottom trace), in 10 mM Tris·HCl (pH 7.8). (*B*) Class 4 suppressor, in 10 mM Tris·HCl (pH 7.8) (top trace) and 10 mM Mes (pH 6.0) (bottom trace). Similar transients recorded with RCs isolated from the strains in *A* have been reported (30); the experiment was repeated with native chromatophores for comparison to other PS^+ derivatives. All traces are single-transient recording, with the exception of the class 4 strain data at pH 6.0 (average of eight transients, 25 s apart).

Double Mutant L212-213AA and PS^+ Derivatives. The position of the protonatable residues Glu-L212 and Asp-L213 in the RC structure (Fig. 1) suggested that they could contribute to the asymmetrical redox properties of ubiquinone$_{10}$ in the Q_B and Q_A sites. Replacement of these acidic residues with Ala residues found at the symmetry-related positions in the Q_A site generated a PS^- strain of *Rb. capsulatus* in which successive electron transfers from Q_A to Q_B are blocked (Fig. 3) because protonation of Q_B^- does not occur (30). These results agree with those obtained for other mutants that have established roles for Glu-L212 and Asp-L213 in the proton transfer network in wild-type RCs of *Rb. sphaeroides* (17–20).

At least five genotypes can restore the RC function lost in the L212-213AA double mutant to yield a photocompetent strain (Table 1). Complementation tests determined that the sequence combinations found in classes 1–4 are indeed responsible for regeneration of the PS^+ phenotype. The growth assays are corroborated by demonstration of quinone oscillations, which show that RCs bearing these sequence changes are capable of cyclic photochemistry. Therefore, the amino acid substitutions found in the PS^+ derivatives restore the proton transfer function that is destroyed by the Ala replacements at L212 and L213. The second-site suppressor mutations show that neither Glu-L212 nor Asp-L213 is essential for this function and demonstrate that alternate proton delivery pathways have been established in these strains as a result of these substitutions.

Compensation for Loss of Glu-L212 and Asp-L213 in Revertant and Suppressor Strains. The PS^+ phenotype of strains in which a nonprotonatable nonpolarizable Ala at L212 is coupled with a protonatable Asp at either L213 or L225 (classes 1 and 2, respectively) shows that reacquisition of one of the protonatable residues lost in the Q_B site of the L212-213AA mutant is one way of restoring RC activity and that this protonatable residue can be located at a second site within the Q_B binding cavity.

The Arg-M231 $\rightarrow$ Leu (class 3) and Asn-M43 $\rightarrow$ Asp (class 4) suppressors show that distant amino acid replacements, which alter the charge distribution of the RC, can also compensate for loss of acidic groups in the Q_B site. The amino acid sequence in the Q_B binding pocket in these PS^+ strains is identical to that of the PS^- double mutant. In RCs of class 3 strains, suppression of the PS^- phenotype is achieved when a basic residue, Arg-M231, is lost rather than by the addition of an acidic residue as seen in classes 1 and 2. The Arg-M231 $\rightarrow$ Leu mutation restores the pK values of residues involved in stabilization of Q_B^- (30). The disruption of the ionic interactions of Arg-M231 with Glu-H125 and Glu-H232 essentially adds a potential negative charge by freeing the acidic residues for participation in other interactions.

In RCs of class 4 strains, suppression of the PS^- phenotype is achieved when a nonprotonatable residue (Ala-L213) is paired with the Asp-M43, analogous to the configuration found in RCs of *Rp. viridis*, *Rs. rubrum*, and *C. aurantiacus* at these sites (Asn-L213/Asp-M43; refs. 12–15). The wild-type RCs of *Rb. capsulatus* and *Rb. sphaeroides* reverse this combination (9–11). Therefore, it is possible that the proton transfer pathway to Q_B in the suppressor strain of *Rb. capsulatus* more closely resembles those of the first three species that cannot employ Asn-L213 as the principal proton donor to Q_B^{2-} (32).

Modeling of the *Rb. sphaeroides* structure suggests that Asn-M43, Glu-H125, and Glu-H232 lie well outside of the shell of amino acids that forms the Q_B binding pocket (Fig. 1; refs. 30 and 32). Asn-M43 is a part of the second layer of residues that surrounds Q_B, and its side chain extends into the charged interface between the L, M, and H subunits. The distances from Asp-M43 to Ser-L223 (6.8 Å) or to Q_B (9.3 Å) would be too great for direct proton transfer via hydrogen

bonding. The protonatable residues Glu-H125 and Glu-H232 are also distant from Ser-L223 (≈16 Å and 20 Å, respectively) and Q_B (≈14 Å and 18 Å, respectively). Direct interaction of any of these residues with Q_B or Ser-L223 could not be achieved unless gross structural rearrangements occurred as a result of these mutations. However, these substitutions do not appreciably affect the rate of transfer of the first electron from Q_A to Q_B (Fig. 2) or RC turnover ability (Fig. 3). Arg-M231 is not a part of either of the two proton transfer pathways proposed by Allen *et al.* (39), nor are Glu-H125 or Glu-H232. Clearly, determination of the mechanisms by which suppression is achieved in these strains depends on a more extensive study of the biophysical properties of their RCs than is presented in this descriptive survey.

Candidates for the chromosomal suppressor(s) in class 5 strains, all of which retain the Ala mutations, could be substitutions in the H chain, which forms part of the lower region of the Q_B binding pocket (40). The *Rb. sphaeroides* structure (3) shows that conserved residues Asp-H172, Arg-H179, and Glu-M230 (9, 41, 42) form an ion-pair interaction similar to that of Glu-H125, Arg-M231, and Glu-H232. Thus, mutation of Arg-H179 to a neutral residue could yield a class 3-like suppressor, adding a potential negative charge within 8–13 Å of Q_B. Other potential single-site mutations in *H* that could add a negative charge near Q_B are Gln-H176 → Glu and Lys-H133 → Glu.

Historically, protein–Q_B interactions were probed by analyzing herbicide-resistant mutants in bacteria, algae, and plants; none of those occur at the Gly-L225, Arg-M231, or Asn-M43 sites. Although the RC structure was known, the level of understanding of it prior to the isolation of these suppressor mutants would not have suggested Gly-L225 and Arg-M231 as likely candidates for site-specific mutagenesis. Molecular modeling suggests that mutation of Gly-L225 to Asp in otherwise wild-type RCs would place two negatively charged side chains (Asp-L213 and Asp-L225) in such proximity that these mutant RCs might not assemble. Therefore, the analysis of RCs that carry spontaneous mutations at L225, M231, and M43 that compensate for site-specific mutations at L212 and L213 should give insight into the electrochemistry at the Q_B site that could not necessarily be derived from the study of spontaneous or site-specific mutations alone.

Our results demonstrate that there can be multiple routes for the transfer of protons within the RC to reduced Q_B and that changes in the charge distribution affect the pathway for Q_B protonation. The potential for alternative proton delivery pathways is predicated on the observations that RCs from different species are structurally and functionally homologous in the absence of complete sequence homology. Some of these interspecies sequence variations near Q_B are mimicked by the mutations carried by the *Rb. capsulatus* suppressor strains. Understanding the conformational elements that lead to these different proton transfer pathways in the reaction center, where it is possible to generate viable mutants that assemble impaired complexes, should provide a model for study of the structural basis of protein-mediated transmembrane proton transport in a variety of less accessible systems.

We thank D. C. Youvan for the gift of the *Rb. capsulatus* deletion strain and plasmids pU29 and pU2922. We also thank P. Sebban, F. J. Stevens, M. C. Thurnauer, and J. R. Norris for helpful discussions and critical readings of the manuscript. This work was supported by the U.S. Department of Energy, Office of Health and Environmental Research, and the Office of Basic Energy Sciences (D.M.T.), under Contract W-31-109-ENG-38, and by Public Health Service Grant GM36598 (C.-H.C. and M.S.).

1. Feher, G., Allen, J. P., Okamura, M. Y. & Rees, D. C. (1989) *Nature (London)* **339**, 111–116.
2. Deisenhofer, J. & Michel, H. (1989) *Science* **245**, 1463–1473.
3. Chang, C.-H., El-Kabbani, O., Tiede, D., Norris, J. & Schiffer, M. (1991) *Biochemistry* **30**, 5352–5360.
4. El-Kabbani, O., Chang, C.-H., Tiede, D., Norris, J. & Schiffer, M. (1991) *Biochemistry* **30**, 5361–5369.
5. Kirmaier, C. & Holten, D. (1987) *Photosynth. Res.* **13**, 225–260.
6. Michel-Beyerle, M. E., Plato, M., Deisenhofer, J., Michel, H., Bixon, M. & Jortner, J. (1988) *Biochim. Biophys. Acta* **932**, 52–70.
7. Crofts, A. R. & Wraight, C. A. (1983) *Biochim. Biophys. Acta* **726**, 9–185.
8. McPherson, P. H., Okamura, M. Y. & Feher, G. (1990) *Biochim. Biophys. Acta* **1016**, 289–292.
9. Youvan, D. C., Bylina, E. J., Alberti, M., Begusch, H. & Hearst, J. E. (1984) *Cell* **37**, 949–957.
10. Williams, J. C., Steiner, L. A., Ogden, R. C., Simon, M. I. & Feher, G. (1983) *Proc. Natl. Acad. Sci. USA* **80**, 6505–6509.
11. Williams, J. C., Steiner, L. A., Feher, G. & Simon, M. I. (1984) *Proc. Natl. Acad. Sci. USA* **81**, 7303–7307.
12. Michel, H., Weyer, K. A., Gruenberg, H., Dunger, I., Oesterhelt, D. & Lottspeich, F. (1986) *EMBO J.* **5**, 1149–1158.
13. Belanger, G., Berard, J., Corriveau, P. & Gingras, G. (1988) *J. Biol. Chem.* **263**, 7632–7638.
14. Ovchinnikov, Y. A., Abdulaev, N. G., Zolotarev, A. S., Shmuckler, B. E., Zargarov, A. A., Kutuzov, M. A., Telezhinskaya, I. N. & Levina, N. B. (1988) *FEBS Lett.* **231**, 237–242.
15. Ovchinnikov, Y. A., Abdulaev, N. G., Shmuckler, B. E., Zargarov, A. A., Kutuzov, M. A., Telezhinskaya, I. N., Levina, N. B. & Zolotarev, A. S. (1988) *FEBS Lett.* **232**, 364–368.
16. Schiffer, M., Chan, C.-K., Chang, C.-H., DiMagno, T. J., Fleming, G. R., Nance, S., Norris, J., Snyder, S., Thurnauer, M., Tiede, D. M. & Hanson, D. K. (1992) in *The Photosynthetic Bacterial Reaction Center II: Structure, Spectroscopy, and Dynamics*, NATO ASI Series, eds. Breton, J. & Vermeglio, A. (Plenum, London), pp. 351–361.
17. Paddock, M. L., Rongey, S. H., Feher, G. & Okamura, M. Y. (1989) *Proc. Natl. Acad. Sci. USA* **86**, 6602–6606.
18. Takahashi, E. & Wraight, C. A. (1990) *Biochim. Biophys. Acta* **1020**, 107–111.
19. Takahashi, E. & Wraight, C. A. (1992) *Biochemistry* **31**, 855–866.
20. Okamura, M. Y. & Feher, G. (1992) *Annu. Rev. Biochem.* **61**, 861–896.
21. Jones, T. A. (1978) *J. Appl. Crystallogr.* **11**, 268–272.
22. Bylina, E. J., Ismail, S. & Youvan, D. C. (1986) *Plasmid* **16**, 175–181.
23. Bylina, E. J., Jovine, R. V. M. & Youvan, D. C. (1989) *Bio/Technology* **7**, 69–74.
24. Kunkel, T. A., Roberts, J. D. & Zakour, R. A. (1987) *Methods Enzymol.* **154**, 367–382.
25. Sambrook, J., Fritsch, E. F. & Maniatis, T. (1989) *Molecular Cloning: A Laboratory Manual* (Cold Spring Harbor Lab. Press, Plainview, NY).
26. Youvan, D. C., Ismail, S. & Bylina, E. J. (1985) *Gene* **33**, 19–30.
27. Simon, R., Priefer, U. & Puhler, A. (1983) *Bio/Technology* **1**, 37–45.
28. Weaver, P. F., Wall, J. D. & Gest, H. (1975) *Arch. Microbiol.* **105**, 207–216.
29. Davidson, E., Prince, R. C., Haith, C. E. & Daldal, F. (1989) *J. Bacteriol.* **171**, 6059–6068.
30. Hanson, D. K., Baciou, L., Tiede, D. M., Nance, S. L., Schiffer, M. & Sebban, P. (1992) *Biochim. Biophys. Acta* **1102**, 260–265.
31. Bylina, E. J. & Youvan, D. C. (1988) *Proc. Natl. Acad. Sci. USA* **85**, 7226–7230.
32. Hanson, D. K., Nance, S. L. & Schiffer, M. (1992) *Photosynth. Res.* **32**, 147–153.
33. Dutton, P. L., Petty, K. M., Bonner, H. S. & Morse, S. D. (1975) *Biochim. Biophys. Acta* **387**, 536–556.
34. Chan, C.-K., Chen, L. X.-Q., DiMagno, T. J., Hanson, D. K., Nance, S. L., Schiffer, M., Norris, J. R. & Fleming, G. R. (1991) *Chem. Phys. Lett.* **176**, 366–372.
35. Vermeglio, A. & Clayton, R. K. (1977) *Biochim. Biophys. Acta* **461**, 159–165.
36. Vermeglio, A., Martinet, T. & Clayton, R. A. (1980) *Proc. Natl. Acad. Sci. USA* **77**, 1809–1813.
37. Tiede, D. M. & Hanson, D. K. (1992) in *The Photosynthetic Bacterial Reaction Center II: Structure, Spectroscopy, and Dynamics*, NATO ASI Series, eds. Breton, J. & Vermeglio, A. (Plenum, London), pp. 341–350.
38. Paddock, M. L., McPherson, P. H., Feher, G. & Okamura, M. Y. (1990) *Proc. Natl. Acad. Sci. USA* **87**, 6803–6807.
39. Allen, J. P., Feher, G., Yeates, T. O., Komiya, H. & Rees, D. C. (1988) *Proc. Natl. Acad. Sci. USA* **85**, 8487–8491.
40. Deisenhofer, J., Epp, O., Miki, K., Huber, R. & Michel, H. (1985) *Nature (London)* **318**, 618–624.
41. Williams, J. C., Steiner, L. A. & Feher, G. (1986) *Proteins Struct. Funct. Genet.* **1**, 312–325.
42. Michel, H., Weyer, K. A., Gruenberg, H. & Lottspeich, F. (1985) *EMBO J.* **4**, 1667–1672.